Low-Complexity Block Turbo Equalization for OFDM Systems in Time-Varying Channels

Kun Fang, *Student Member, IEEE*, Luca Rugini, *Member, IEEE*, and Geert Leus, *Senior Member, IEEE*

***Abstract*—We propose low-complexity block turbo equalizers for orthogonal frequency-division multiplexing (OFDM) systems in time-varying channels. The presented work is based on a soft minimum mean-squared error (MMSE) block linear equalizer (BLE) that exploits the banded structure of the frequency-domain channel matrix, as well as a receiver window that enforces this banded structure. This equalization approach allows us to implement the proposed designs with a complexity that is only linear in the number of subcarriers. Three block turbo equalizers are discussed: two are based on a biased MMSE criterion, while the third is based on the unbiased MMSE criterion. Simulation results show that the proposed iterative MMSE BLE achieves a better bit error rate (BER) performance than a previously proposed iterative MMSE serial linear equalizer (SLE). The proposed equalization algorithms are also tested in the presence of channel estimation errors.**

***Index Terms*—Intercarrier interference, orthogonal frequency-division multiplexing (OFDM), time-varying channels, turbo equalization.**

I. Introduction

ORTHOGONAL frequency-division multiplexing (OFDM) is one of the most important modulation schemes for wireless communications, since it is widely used in many standards such as DVB-T/H, DAB, IEEE 802.11 and IEEE 802.16 [1], [2]. OFDM can eliminate intersymbol interference (ISI) introduced by a frequency-selective channel by turning it into a set of parallel frequency-flat channels, and therefore renders simple one-tap equalization for each subcarrier [3]. However, high-mobility terminals and scatterers induce a different Doppler shift on each propagation path, giving rise to a time-selective or time-varying channel, thereby destroying the orthogonality among subcarriers. The related intercarrier interference (ICI) severely degrades the performance of the one-tap equalizer [1], [2], [4]. As a consequence, to reduce the performance degradation, OFDM systems in high-mobility scenarios should adopt smarter equalization techniques based on ICI mitigation.

In order to counteract the effects of a time-varying channel, several different equalization techniques have been proposed [5]–[18]. These techniques range from linear equalizers, based on the zero-forcing (ZF) or the minimum mean-squared error (MMSE) criterion [5]–[14], to decision-directed equalizers based on decision-feedback or ICI cancellation [10]–[15]. Also near maximum-likelihood approaches have been proposed [17], [18]. ICI cancellation with transmitter optimization is proposed in [16]. Similar to the situation in single-carrier communications subject to ISI channels, or in multiuser detection for code-division multiple-access (CDMA), each equalization technique is characterized by a different performance-complexity tradeoff. However, the specific structure of the Doppler-induced ICI in OFDM systems presents some distinctive features that can be exploited by the equalizer. The first feature is the limited support of the Doppler spread. References [7]–[11] exploit the banded character of the frequency-domain channel matrix to reach a complexity that is only linear in the number of subcarriers. This is in contrast with more complex equalization methods that rely on the full (i.e., nonbanded) frequency-domain channel matrix. Indeed, for nonbanded methods, the complexity is quadratic [14] or even cubic [13] in the number of subcarriers, and therefore can be too high for standards with a large number of subcarriers like DVB. In a certain sense, the assumption of a banded frequency-domain channel matrix is a natural extension of the time-invariant channel case, where the frequency-domain channel matrix is diagonal and hence banded with the smallest possible bandwidth. A second feature that can be exploited in the equalization is the knowledge of the Doppler spectrum shape, typically a U-shaped spectrum, a bell-shaped spectrum, or a combination thereof. This knowledge can be used to design simple time-domain receiver windows that enforce the banded assumption and improve the performance of equalization schemes [10], [11].

Among all the equalizers for OFDM in time-varying channels, one of the most promising approaches is the iterative MMSE serial linear equalizer (SLE) of [10]. This iterative approach is inspired by turbo equalization [19], [20], where soft information is used in an iterative fashion to improve the bit error rate (BER) performance, and it will therefore also be labeled as the serial turbo MMSE equalizer in the sequel. Optimal joint processing of equalization and decoding at the

Manuscript received July 24, 2007; revised July 3, 2008. First published August 1, 2008; current version published October 15, 2008. The associate editor coordinating the review of this paper and approving it for publication was Dr. Gerald Matz. This research was supported in part by NWO-STW under the VIDI program (DTC.6577) and VICI program (DTC.5893). This paper was presented in part at the International Conference on Acoustics, Speech and Signal Processing, Honolulu, HI, April 2007.

K. Fang and G. Leus are with the Faculty of Electrical Engineering, Mathematics and Computer Science (EEMCS), Delft University of Technology, 2628 CD Delft, The Netherlands (e-mail: k.fang@tudelft.nl, g.j.t.leus@tudelft.nl).

L. Rugini was with the Faculty of Electrical Engineering, Mathematics and Computer Science (EEMCS), Delft University of Technology, 2628 CD Delft, The Netherlands. He is now with the Dipartimento di Ingegneria Elettronica e dell'Informazione (DIEI), the University of Perugia, Perugia 06125, Italy (e-mail: luca.rugini@diei.unipg.it).

Color versions of one or more of the figures in this paper are available online at http://ieeexplore.ieee.org.

Digital Object Identifier 10.1109/TSP.2008.929129

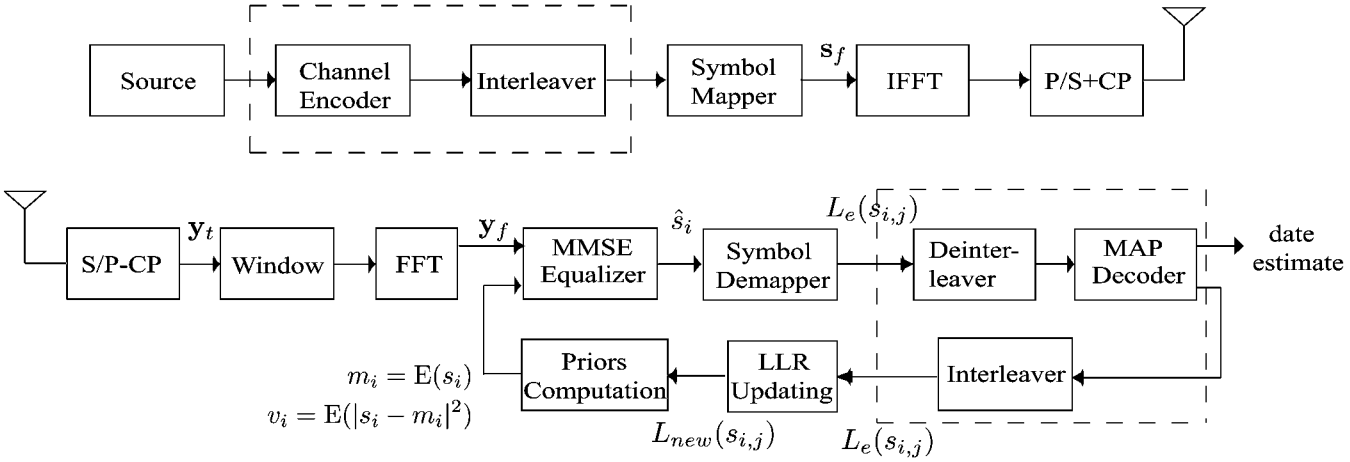

Fig. 1. System model for the proposed block turbo equalizers.

receiver is prohibitive due to the heavy computational burden. Instead, the equalization and decoding tasks can be performed separately and carried out iteratively, with soft information being interchanged between these two parts. For example, turbo MMSE equalizers iteratively improve the mean and the covariance of the estimated symbol vector by exploiting extrinsic information and performing soft cancellation. Different turbo MMSE equalizers exist in the technical literature, such as serial or block versions [19]–[22]. The difference between a serial and a block approach is that in the serial case each symbol is equalized separately using a sliding window MMSE equalizer [19], [20], whereas in the block case all the symbols in a block are jointly equalized [21], [22].

In this paper, we derive *block* turbo MMSE equalizers for OFDM systems in time-varying channels, as an alternative to the *serial* turbo MMSE equalization [10]. The presented equalizers are based on a soft MMSE block linear equalizer (BLE), and exploit both the banded structure of the frequency-domain channel matrix and receiver windowing. Therefore, their complexities will be linear in the number of subcarriers, like the methods in [7]–[11]. Three different algorithms are proposed, and their complexities are investigated. In addition, we establish some insightful mutual relations among the different methods as well as connections to existing turbo methods. The performances of the proposed block turbo MMSE equalizers are compared with that of the serial turbo MMSE equalizer of [10]. In [11], it has been shown that the noniterative block MMSE equalizer outperforms the noniterative serial MMSE equalizer. The simulation results in this paper will display that their iterative versions have a similar performance difference. Specifically, our block equalizers are able to reduce the error floor of the BER performance due to the ICI. In order to establish a fair comparison with [10], we do not consider channel coding at first. However, it is clear that the performance can be further improved by incorporating error correction codes into the turbo loop. This is also illustrated in the simulations section.

The Doppler shift caused by the high mobility also makes the channel estimation problem more challenging. The turbo equalization algorithms developed in this paper assume that the receiver has perfect channel state information (CSI) and the transmitter has no access to CSI. In practice, the equalizer can use an estimated CSI, obtained for instance by using the techniques developed in [23], as we will show in the simulations section. Further improvements, beyond the scope of this paper, could be obtained by exploiting some knowledge about the channel estimation error [21] or by incorporating channel estimation into the iterative equalization and decoding loop [24].

The rest of the paper is organized as follows. In Section II, we briefly introduce the system model. In Section III, we present the three proposed block turbo MMSE equalizers. In Section IV, we mainly focus on their similarities and differences, as well as on connections to other block turbo methods. Section V deals with computational complexity issues and shows how the proposed equalizers can be implemented with low complexity. In Section VI, we evaluate the performance of our equalizers by simulation, also in the presence of channel estimation errors and channel coding. We conclude the paper in Section VII.

Notation: We use upper (lower) boldface letters to denote matrices (column vectors). $(\cdot)^T$ and $(\cdot)^H$ represent transpose and complex conjugate transpose (Hermitian), respectively. $[\mathbf{A}]_{m,n}$ indicates the entry in the mth row and nth column of $\mathbf{A}$. We use the symbol $\circ$ to denote the Hadamard (element-wise) product between matrices. $\mathrm{diag}(\mathbf{a})$ is a diagonal matrix with the vector $\mathbf{a}$ on the diagonal. $E(\cdot)$ stands for the statistical expectation. The covariance matrix between $\mathbf{x}$ and $\mathbf{y}$ is defined as $\mathrm{Cov}(\mathbf{x},\mathbf{y}) = E(\mathbf{x}\mathbf{y}^H) - E(\mathbf{x})E(\mathbf{y}^H)$. Finally, $\mathbf{0}_{M\times N}$ and $\mathbf{I}_N$ denote the $M \times N$ all-zero matrix and the $N \times N$ identity matrix, respectively.

II. System Model

We consider a single-user OFDM system with N subcarriers, over a channel that is both frequency and time selective. The structure of the transmitter and the receiver is shown in Fig. 1. As already discussed in the introduction, we will mainly focus on the equalization part in this paper, rather than on the (de)coding part. Hence, we start by omitting the channel

TABLE I
QPSK SYMBOL ALPHABET

k	1	2	3	4
$(\alpha_{k,1}, \alpha_{k,2})$	(0,0)	(1,0)	(0,1)	(1,1)
α_k	$\frac{(+1+i)}{\sqrt{2}}$	$\frac{(-1+i)}{\sqrt{2}}$	$\frac{(+1-i)}{\sqrt{2}}$	$\frac{(-1-i)}{\sqrt{2}}$

(de)coder (dashed boxes in Fig. 1) when explaining the basic ideas. In the simulations section, however, we will also present some results with channel coding, for which the decoder is included in the turbo loop. At the transmitter, the bits are grouped and mapped into complex symbols. For simplicity, we consider quaternary phase-shift keying (QPSK) with the symbol alphabet shown in Table I. However, the equalizers proposed herein can be easily extended to other constellations like in [20]. As far as the time-dispersion of the channel is concerned, we adopt the standard assumption that the channel delay spread is smaller than the OFDM cyclic prefix (CP) length L. This way, there is no interference between successive OFDM blocks, and the equalizer can be designed separately for each OFDM block. For this reason, we omit the OFDM block index from our notation. At the receiver, after removing the CP, the $N \times 1$ time-domain received vector $\mathbf{y}_t$ can be expressed as

$$\mathbf{y}_t = \mathbf{H}_t \mathbf{F}^H \mathbf{s}_f + \mathbf{n}_t \tag{1}$$

where $\mathbf{H}_t$ is the $N \times N$ time-domain channel matrix, $\mathbf{F}$ denotes the $N \times N$ unitary DFT matrix, $\mathbf{s}_f$ represents the $N \times 1$ OFDM symbol, and $\mathbf{n}_t$ stands for the $N \times 1$ noise vector. For simplicity, we assume that $\mathbf{n}_t$ is a circularly symmetric complex Gaussian noise vector, with zero mean and covariance $E\{\mathbf{n}_t \mathbf{n}_t^H\} = \sigma_n^2 \mathbf{I}_N$. A more detailed baseband-equivalent channel description can be found in [5].

At the receiver, a time-domain window can be applied after the CP removal and before the FFT operation. In this case, the output vector after the FFT operation can be expressed as

$$\mathbf{y}_f = \mathbf{F}\mathbf{W}\mathbf{H}_t\mathbf{F}^H\mathbf{s}_f + \mathbf{F}\mathbf{W}\mathbf{n}_t = \mathbf{H}_f\mathbf{s}_f + \mathbf{n}_f \tag{2}$$

where $\mathbf{y}_f = \mathbf{F}\mathbf{W}\mathbf{y}_t$, $\mathbf{n}_f = \mathbf{F}\mathbf{W}\mathbf{n}_t$, $\mathbf{H}_f = \mathbf{F}\mathbf{W}\mathbf{H}_t\mathbf{F}^H$, and $\mathbf{W} = \mathrm{diag}(\mathbf{w})$, with $\mathbf{w}$ denoting the time-domain receiver window. Note that classical OFDM does not include windowing, i.e., $\mathbf{W} = \mathbf{I}_N$.

When the channel is time-invariant and no windowing is employed, i.e., $\mathbf{W} = \mathbf{I}_N$, the time-domain channel matrix $\mathbf{H}_t$ is circulant, and consequently the frequency-domain channel matrix $\mathbf{H}_f$ is diagonal. This triggers the use of the simple traditional OFDM one-tap equalizer. However, in a time-varying scenario, $\mathbf{H}_t$ is no longer circulant, and $\mathbf{H}_f$ becomes a nondiagonal matrix, giving rise to ICI that corresponds to the nonzero off-diagonal elements of $\mathbf{H}_f$. Fortunately, $\mathbf{H}_f$ is almost banded, with the most significant elements around the main diagonal [8]. This permits the use of low-complexity equalization, as explained in [8]–[11]. The banded structure turns out to be very useful, since easy equalization is one of the main advantages of OFDM over single-carrier communications. Moreover, with an appropriate window design $\mathbf{W}$, the banded character of $\mathbf{H}_f = \mathbf{F}\mathbf{W}\mathbf{H}_t\mathbf{F}^H$ can even be enforced. This means that the neglected ICI, corresponding to the out-of-band elements of $\mathbf{H}_f$, has a smaller power, leading to equalizers with improved performance [10], [11].

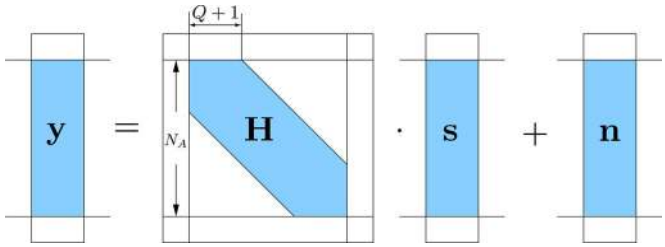

Fig. 2. System input–output relation after removing the guard intervals.

As in [9], [11], we assume that the OFDM symbol $\mathbf{s}_f$ is constructed as $\mathbf{s}_f = [\mathbf{0}_{N_V/2\times 1}^T, \mathbf{s}^T, \mathbf{0}_{N_V/2\times 1}^T]^T$, where the $N_V/2 \times 1$ all-zero vectors represent frequency-domain guard bands and the $N_A \times 1$ vector $\mathbf{s}$ is the actual data vector (note that $N = N_A + N_V$). Although these guard bands do not correspond exactly to the edge frequencies, it is easy to imagine that by circularly shifting the columns of the unitary DFT matrix $\mathbf{F}$, they can be envisioned as being the edge frequencies. In this context, the motivation for guard bands in the frequency domain is twofold. First, guard bands prevent adjacent channel interference, and hence their use is widely adopted in many OFDM standards [1], [2]. Second, in the considered time-varying setup, guard bands also eliminate the cross-coupling between the subcarriers that are located at the edge frequencies. This translates into relevant elements in the top-right and bottom-left corners of $\mathbf{H}_f$, as shown in [10]. By using guard bands at the transmitter, we can remove these unwanted corners. For simplicity reasons, we also remove the first and the last $N_V/2$ entries of $\mathbf{y}_f$ at the receiver, and only focus on the N_A middle entries. Hence, introducing the matrix $\mathbf{S} = [\mathbf{0}_{N_A\times N_V/2}, \mathbf{I}_{N_A}, \mathbf{0}_{N_A\times N_V/2}]$, which selects the $N_A \times 1$ middle block out of an $N \times 1$ vector, we transform (2) into

$$\mathbf{y} = \mathbf{H}\mathbf{s} + \mathbf{n} \tag{3}$$

where $\mathbf{y} = \mathbf{S}\mathbf{y}_f$, $\mathbf{s} = \mathbf{S}\mathbf{s}_f$, $\mathbf{n} = \mathbf{S}\mathbf{n}_f$, and $\mathbf{H} = \mathbf{S}\mathbf{H}_f\mathbf{S}^H$, which represents the $N_A \times N_A$ middle block of the frequency-domain channel matrix $\mathbf{H}_f$, as shown in Fig. 2. To simplify equalization, the matrix $\mathbf{H}$ is further approximated by its banded version

$$\mathbf{B} = \mathbf{H} \circ \mathbf{\Theta}_Q \tag{4}$$

where $\mathbf{\Theta}_Q$ is the $N_A \times N_A$ Toeplitz matrix with entries defined as $[\mathbf{\Theta}_Q]_{m,n} = 1$ for $|m-n| \leq Q$ and $[\mathbf{\Theta}_Q]_{m,n} = 0$ for $|m-n| > Q$. The bandwidth parameter Q is used to control how many off-diagonal elements should be included to have a good banded approximation of the frequency-domain channel matrix. Tuning Q allows for a tradeoff between equalizer complexity and performance. The parameter Q can be chosen according to some rules of thumb [10]. When windowing is included, it is usually much smaller than the number of subcarriers N, e.g., $1 \leq Q \leq 4$. Note that Q also determines the design of the window $\mathbf{W}$ [10], [11].

III. Block Turbo MMSE Equalization

In this section, we derive three block turbo MMSE equalizers for OFDM subject to time-varying channels, relying on the banded approximation expressed by (4). The transmission system groups $2N_A$ bits to form an OFDM symbol $\mathbf{s} = [s_1, s_2, \ldots, s_{N_A}]^T$, where $s_i \in \{\alpha_k : k = 1, \ldots, 4\}$ is the QPSK symbol on the ith active subcarrier, and $(s_{i,1}, s_{i,2}) \in \{(\alpha_{k,1}, \alpha_{k,2}) : k = 1, \ldots, 4\}$ are the related bits (see Table I). The information bits are assumed to be independent and identically distributed (i.i.d.).

A turbo MMSE equalizer is a Bayesian iterative equalizer obtained by exploiting some prior knowledge about the symbols to be estimated. This prior knowledge is represented by the means $m_i = E(s_i)$ and the variances $v_i = E\left(|s_i - m_i|^2\right)$ of the symbols to be estimated. At the beginning, when prior information is not available, $m_i = 0$ and $v_i = 1$ for all the N_A symbols. After equalization, these means and variances are updated by using soft information from the estimated symbols, i.e., from the symbols obtained at the equalizer output. More specifically, the calculation of the mean m_i and the variance v_i relies on soft information represented by a log-likelihood ratio (LLR) at the bit level. Hence, focusing on the bit $s_{i,j}$, we define the *a priori* LLR, the *a posteriori* LLR, and the *extrinsic* LLR, respectively as [19]

$$\begin{aligned} L(s_{i,j}) &= \ln \frac{P(s_{i,j}=0)}{P(s_{i,j}=1)}, \\ L(s_{i,j}|\hat{s}_i) &= \ln \frac{P(s_{i,j}=0|\hat{s}_i)}{P(s_{i,j}=1|\hat{s}_i)}, \\ L_e(s_{i,j}) &= L(s_{i,j}|\hat{s}_i) - L(s_{i,j}) \\ &= \ln \frac{\sum_{\alpha_k:\alpha_{k,j}=0} p(\hat{s}_i|s_i=\alpha_k) P(s_{i,j'}=\alpha_{k,j'})}{\sum_{\alpha_k:\alpha_{k,j}=1} p(\hat{s}_i|s_i=\alpha_k) P(s_{i,j'}=\alpha_{k,j'})} \end{aligned} \tag{5}$$

where $j, j' = 1, 2$, with $j \neq j'$, and $\hat{s}_i$ is the estimated symbol at the current iteration. It is clear that the *a priori* LLR is available before the equalization, whereas the *a posteriori* LLR is obtained after equalization by adding the extrinsic LLR to the *a priori* LLR. Hence, the extrinsic LLR represents the new amount of information on the bits furnished by the current equalizer iteration. Then, the *a posteriori* LLR for the current iteration is used as *a priori* LLR for the next iteration, which will be denoted by L_{new}. We observe that, in our definition, the *a posteriori* LLR of the bit $s_{i,j}$ is conditioned only on the symbol $\hat{s}_i$ rather than on the entire estimated OFDM symbol. This simplification, which is the same as in [20], allows for an easier evaluation of the extrinsic LLR. Then, for each subcarrier i, the two new LLR's (one for each bit) are combined to obtain an updated version of the *a priori* mean and variance of the estimated symbol, which will be denoted by $m_{i,\text{new}}$ and $v_{i,\text{new}}$, respectively. In summary, each iteration of a block turbo MMSE equalizer can be split into three steps: i) a linear MMSE equalizer is constructed using prior means and variances, and it is applied to the received vector (equalization step); ii) new LLR values are calculated from the equalizer output (LLR updating step); and iii) the means and variances of the estimated symbols are updated using the new LLR values (priors computation step).

A. Block Turbo Equalizer I

The first equalizer we propose, which will be called *equalizer I*, is based on a linear MMSE criterion that produces biased symbol estimates. We adopt the subscript *I* to denote quantities obtained by this equalizer.

Using *a priori* information $\mathbf{m}_I = [m_{I,1}, m_{I,2}, \ldots, m_{I,N_A}]^T$ and $\mathbf{V}_I = \text{diag}\left([v_{I,1}, v_{I,2}, \ldots, v_{I,N_A}]^T\right)$, the linear MMSE estimate of the symbol on the ith subcarrier is given by [25]

$$\hat{s}_{I,i} = m_{I,i} + \mathbf{g}_{I,i}^H(\mathbf{y} - \mathbf{B}\mathbf{m}_I) \tag{6}$$

$$\mathbf{g}_{I,i} = v_{I,i}\mathbf{A}_I^{-1}\mathbf{b}_i \tag{7}$$

where

$$\mathbf{A}_I = \mathbf{B}\mathbf{V}_I\mathbf{B}^H + \mathbf{R}_\mathbf{n} \tag{8}$$

with $\mathbf{b}_i$ being the ith column of $\mathbf{B}$, and $\mathbf{R}_\mathbf{n} = E\{\mathbf{n}\mathbf{n}^H\} = \sigma_n^2\mathbf{S}\mathbf{F}\mathbf{W}\mathbf{W}^H\mathbf{F}^H\mathbf{S}^H$ representing the frequency-domain noise covariance matrix. In the first iteration, when no *a priori* information is available, we have $m_{I,i} = 0$ and $v_{I,i} = 1$, and the equalizer becomes the noniterative MMSE BLE of [11].

After the equalization, the next step is the extrinsic LLR updating. To perform this calculation, we should derive the probability density function (PDF) $p(\hat{s}_{I,i}|s_i = \alpha_k)$. In general, the exact derivation of this PDF is not easy. However, the PDF $p(\hat{s}_{I,i}|s_i = \alpha_k)$ can be approximated as Gaussian, with mean $\mu_{I,i,k}$ and variance $\sigma_{I,i,k}^2$. This approximation is extensively used in turbo equalization, because it highly simplifies the LLR updating (see, e.g., [19]). Note that this choice is not only made for convenience reasons. In a CDMA scenario, the results presented in [26] clearly show that the random variables at the output of a linear MMSE estimator are quite close to be Gaussian distributed. Since our OFDM system can be viewed as a special case of a CDMA system, where each carrier acts as a user, we may assume that the Gaussian approximation also holds in our case. Therefore, $p(\hat{s}_{I,i}|s_i = \alpha_k)$ can be written as

$$\begin{aligned} p(\hat{s}_{I,i}|s_i=\alpha_k) &= \frac{1}{\pi\sigma_{I,i,k}^2} \cdot e^{-|\hat{s}_{I,i}-\mu_{I,i,k}|^2/\sigma_{I,i,k}^2}, \\ \mu_{I,i,k} &= E(\hat{s}_{I,i}|s_i=\alpha_k) \\ &= m_{I,i} + \mathbf{g}_{I,i}^H\mathbf{b}_i(\alpha_k - m_{I,i}) \\ &= m_{I,i} + v_{I,i}t_{I,i}(\alpha_k - m_{I,i}), \\ \sigma_{I,i,k}^2 &= \text{Cov}(\hat{s}_{I,i}, \hat{s}_{I,i}|s_i=\alpha_k) \\ &= \mathbf{g}_{I,i}^H\text{Cov}(\mathbf{y}, \mathbf{y}|s_i=\alpha_k)\mathbf{g}_{I,i} \\ &= \mathbf{g}_{I,i}^H\left(\mathbf{B}\mathbf{V}_I\mathbf{B}^H + \mathbf{R}_\mathbf{n} - v_{I,i}\mathbf{b}_i\mathbf{b}_i^H\right)\mathbf{g}_{I,i} \\ &= v_{I,i}\mathbf{b}_i^H\left(\mathbf{B}\mathbf{V}_I\mathbf{B}^H + \mathbf{R}_\mathbf{n}\right)^{-1} \\ &\quad \times \left(\mathbf{B}\mathbf{V}_I\mathbf{B}^H + \mathbf{R}_\mathbf{n} - v_{I,i}\mathbf{b}_i\mathbf{b}_i^H\right) \\ &\quad \times \left(\mathbf{B}\mathbf{V}_I\mathbf{B}^H + \mathbf{R}_\mathbf{n}\right)^{-1}\mathbf{b}_i v_{I,i} \\ &= v_{I,i}^2 t_{I,i}(1 - v_{I,i}t_{I,i}) \end{aligned} \tag{9}$$

with

$$t_{I,i} = \mathbf{b}_i^H(\mathbf{B}\mathbf{V}_I\mathbf{B}^H + \mathbf{R}_\mathbf{n})^{-1}\mathbf{b}_i. \tag{10}$$

Based on the above equations, the extrinsic information can be calculated from (5), as detailed in the Appendix , which leads to the following result:

$$L_e(s_{I,i,1}) = \frac{\sqrt{8}\mathrm{Re}(\hat{s}_{I,i} - m_{I,i}(1 - v_{I,i}t_{I,i}))}{v_{I,i}(1 - v_{I,i}t_{I,i})}$$
$$L_e(s_{I,i,2}) = \frac{\sqrt{8}\mathrm{Im}(\hat{s}_{I,i} - m_{I,i}(1 - v_{I,i}t_{I,i}))}{v_{I,i}(1 - v_{I,i}t_{I,i})}. \quad (11)$$

Now we are ready to continue with the priors computation step. The extrinsic LLR is added to the *a priori* LLR to form the *a posteriori* LLR or the new version of the *a priori* LLR, which is used to update the means and the variances of the estimated symbol as in [20]

$$L_{\mathrm{new}}(s_{I,i,j}) = L(s_{I,i,j}) + L_e(s_{I,i,j})$$
$$m_{I,i,\mathrm{new}} = \frac{\tanh\left(\frac{L_{\mathrm{new}}(s_{I,i,1})}{2}\right) + i \cdot \tanh\left(\frac{L_{\mathrm{new}}(s_{I,i,2})}{2}\right)}{\sqrt{2}}$$
$$v_{I,i,\mathrm{new}} = 1 - |m_{I,i,\mathrm{new}}|^2. \quad (12)$$

Summarizing, equalizer I calculates the estimate of the entire OFDM symbol $\{\hat{s}_{I,i}, i = 1, \ldots, N_A\}$ according to (6)–(7), and then the priors are calculated using (11)–(12). The whole procedure described in this subsection can then be repeated, depending on the chosen number of iterations.

B. Block Turbo Equalizer II

In turbo equalization and turbo decoding, it is a good rule to have the extrinsic information $L_e(s_{i,j})$ independent from the *a priori* LLR $L(s_{i,j})$ [19], [20]. Indeed, the extrinsic information represents only the new information gained by equalization, and should not depend on the *a priori* LLR, which is added separately during the LLR update. In the previous equalizer, however, the estimated symbol $\hat{s}_{I,i}$ depends on the *a priori* mean $m_{I,i}$ and variance $v_{I,i}$. Therefore, in our equalizer I, the prior knowledge is in a certain way overrated, because it also contributes to the extrinsic LLR. In this subsection, we modify the previously proposed equalizer to make the extrinsic LLR independent from the *a priori* LLR. To achieve this goal, we design our *equalizer II* in such a way that the equalizer output $\hat{s}_{II,i}$ at the ith subcarrier is independent from the specific values of $m_{II,i}$ and $v_{II,i}$ [19]. In this way, the extrinsic LLR $L_e(s_{II,i,j})$, which is obtained from the equalizer output at the ith subcarrier, does not depend on the prior knowledge of the specific ith QPSK symbol, but depends only on the prior knowledge of the QPSK symbols with indexes $\{i' : i' \neq i\}$.

To obtain a mathematical expression for equalizer II, let us recall the equalizer I expressions (6) and (7), derived in the previous subsection. In order to make the estimated symbol on the ith subcarrier independent from the prior knowledge of the ith symbol itself, we should set $m_{II,i}$ equal to zero and $v_{II,i}$ equal to one. However, when estimating the symbols on the other subcarriers, we should maintain $m_{II,i}$ and $v_{II,i}$ equal to their original values, obtained from the previous iteration. To achieve these two requirements, we adopt a similar modification as in [19], and we express the equalizer as

$$\hat{s}_{II,i} = \mathbf{g}_{II,i}^H(\mathbf{y} - \mathbf{B}\mathbf{m}_{II} + m_{II,i}\mathbf{b}_i) \quad (13)$$
$$\mathbf{g}_{II,i} = \left(\mathbf{A}_{II} + (1 - v_{II,i})\mathbf{b}_i\mathbf{b}_i^H\right)^{-1}\mathbf{b}_i \quad (14)$$

where $\mathbf{A}_{II}$ is similarly defined as in (8). At a first look, this block MMSE equalizer seems much more complicated than the first one, because a matrix inverse for each subcarrier is required in (13), whereas a single inverse is shared by all the subcarriers in (6). However, it is possible to show that also equalizer II can use a unique shared inverse. Indeed, from the matrix inversion lemma, we obtain

$$\left(\mathbf{A}_{II} + (1 - v_{II,i})\mathbf{b}_i\mathbf{b}_i^H\right)^{-1} = \mathbf{A}_{II}^{-1} - \frac{1 - v_{II,i}}{1 + (1 - v_{II,i})t_{II,i}}\mathbf{A}_{II}^{-1}\mathbf{b}_i\mathbf{b}_i^H\mathbf{A}_{II}^{-1} \quad (15)$$

where $t_{II,i}$ is similarly defined as in (10). Consequently, $\mathbf{g}_{II,i}$ becomes

$$\mathbf{g}_{II,i} = \mathbf{A}_{II}^{-1}\mathbf{b}_i - \frac{1 - v_{II,i}}{1 + (1 - v_{II,i})t_{II,i}}t_{II,i}\mathbf{A}_{II}^{-1}\mathbf{b}_i = \frac{1}{1 + (1 - v_{II,i})t_{II,i}}\mathbf{A}_{II}^{-1}\mathbf{b}_i. \quad (16)$$

Hence, from (13), the estimated symbol becomes

$$\hat{s}_{II,i} = \frac{1}{1 + (1 - v_{II,i})t_{II,i}}\mathbf{b}_i^H\mathbf{A}_{II}^{-1}(\mathbf{y} - \mathbf{B}\mathbf{m}_{II}) + \frac{t_{II,i}m_{II,i}}{1 + (1 - v_{II,i})t_{II,i}}. \quad (17)$$

From (17), it is clear that the same inverse $\mathbf{A}_{II}^{-1}$ can be used for every subcarrier. Hence, the structure of equalizer II is quite similar to that of equalizer I. We highlight that a similar procedure has also been presented in [22] but in a CDMA context. The main difference with [22] is that we are using an alternative expression for the MMSE equalizer.

Also the LLR calculation can be derived similarly to that for equalizer I. The PDF $p(\hat{s}_{II,i}|s_i = \alpha_k)$ is again assumed Gaussian, with mean and variance expressed by

$$\mu_{II,i,k} = \frac{1}{1 + (1 - v_{II,i})t_{II,i}}t_{II,i}\alpha_k$$
$$\sigma_{II,i,k}^2 = \mathbf{g}_{II,i}^H(\mathbf{B}\mathbf{V}_{II}\mathbf{B}^H - v_{II,i}\mathbf{b}_i\mathbf{b}_i^H + \mathbf{R}_{\mathbf{n}})\mathbf{g}_{II,i} = \frac{1}{[1 + (1 - v_{II,i})t_{II,i}]^2}t_{II,i}(1 - v_{II,i}t_{II,i}). \quad (18)$$

Therefore, by using the same procedure of the Appendix for Equalizer I, the extrinsic LLR can be calculated as

$$L_e(s_{II,i,1}) = \frac{[1 + (1 - v_{II,i})t_{II,i}]\sqrt{8}\mathrm{Re}(\hat{s}_{II,i})}{1 - v_{II,i}t_{II,i}}$$
$$L_e(s_{II,i,2}) = \frac{[1 + (1 - v_{II,i})t_{II,i}]\sqrt{8}\mathrm{Im}(\hat{s}_{II,i})}{1 - v_{II,i}t_{II,i}}. \quad (19)$$

The update of the means and variances of the symbol estimates is the same as in (12).

C. Block Turbo Equalizer III

The two previous equalizers are biased, since $E\{\hat{s}_i\} \neq s_i$. However, an unbiased equalizer can be derived by simply removing the bias term from equalizer I or equalizer II, as done in [27] for a decision-feedback equalizer. From (6), we observe that the bias term for equalizer I can be expressed by

$$E(\hat{s}_{I,i}) - s_i = m_{I,1} + (v_{I,i}t_{I,i} - 1)s_i - m_{I,i}v_{I,i}t_{I,i} \quad (20)$$

and, from (17), the bias for equalizer II is

$$E(\hat{s}_{II,i}) - s_i = \left(\frac{t_{II,i}}{1 + (1 - v_{II,i})t_{II,i}} - 1\right) s_i. \quad (21)$$

Please observe that $E(\hat{s}_{I,i})$ and $E(\hat{s}_{II,i})$ are *a posteriori* expected values performed after equalization, and should not be confused with the *a priori* means $m_{I,i} = E(s_{I,i})$ and $m_{II,i} = E(s_{II,i})$, which are the corresponding expected values before equalization. By compensating for the bias, we obtain one and the same expression for the unbiased equalizer, which we call *equalizer III*. More specifically, for equalizer I and II, the ith unbiased estimated symbol can be written as

$$\frac{\hat{s}_{I,i} - (1 - v_{I,i}t_{I,i})m_{I,i}}{v_{I,i}t_{I,i}} \text{ and } \frac{1 + (1 - v_{II,i})t_{II,i}}{t_{II,i}}\hat{s}_{II,i} \quad (22)$$

respectively, which both lead to the following expression:

$$\hat{s}_{III,i} = \frac{1}{t_{III,i}}\mathbf{b}_i^H \mathbf{A}_{III}^{-1}(\mathbf{y} - \mathbf{B}\mathbf{m}_{III}) + m_{III,i} \quad (23)$$

where $t_{III,i}$ and $\mathbf{A}_{III}$ are similarly defined as in (10) and (8), respectively. The mean and variance can be expressed by

$$\begin{aligned} \mu_{III,i,k} &= \alpha_k \\ \sigma^2_{III,i,k} &= \frac{1 - v_{III,i}t_{III,i}}{t_{III,i}}. \end{aligned} \quad (24)$$

The extrinsic information can be calculated in the same way as in (11) or (19), leading to

$$\begin{aligned} L_e(s_{III,i,1}) &= \frac{t_{III,i}\sqrt{8}\mathrm{Re}(\hat{s}_{III,i})}{1 - v_{III,i}t_{III,i}} \\ L_e(s_{III,i,2}) &= \frac{t_{III,i}\sqrt{8}\mathrm{Im}(\hat{s}_{III,i})}{1 - v_{III,i}t_{III,i}}. \end{aligned} \quad (25)$$

The means and variances of the symbol estimates can then again be updated as in (12).

IV. Comparisons

We now compare the extrinsic LLRs of the three equalizers by inserting (6), (17), and (23), into (11), (19), and (25), respectively. By focusing on the first bit of subcarrier i, we obtain

$$\begin{aligned} L_e(s_{I,i,1}) = \sqrt{8}\mathrm{Re}\Bigg[& \frac{1}{1 - v_{I,i}t_{I,i}}\mathbf{b}_i^H \mathbf{A}_I^{-1}(\mathbf{y} - \mathbf{B}\mathbf{m}_I) \\ & + \frac{m_{I,i}}{v_{I,i}(1 - v_{I,i}t_{I,i})} - \frac{m_{I,i}}{v_{I,i}}\Bigg] \end{aligned}$$

$$\begin{aligned} L_e(s_{II,i,1}) = \sqrt{8}\mathrm{Re}\Bigg[& \frac{1}{1 - v_{II,i}t_{II,i}}\mathbf{b}_i^H \mathbf{A}_{II}^{-1}(\mathbf{y} - \mathbf{B}\mathbf{m}_{II}) \\ & + \frac{t_{II,i}m_{II,i}}{1 - v_{II,i}t_{II,i}}\Bigg], \end{aligned}$$

$$\begin{aligned} L_e(s_{III,i,1}) = \sqrt{8}\mathrm{Re}\Bigg[& \frac{1}{1 - v_{III,i}t_{III,i}}\mathbf{b}_i^H \mathbf{A}_{III}^{-1}(\mathbf{y} - \mathbf{B}\mathbf{m}_{III}) \\ & + \frac{t_{III,i}m_{III,i}}{1 - v_{III,i}t_{III,i}}\Bigg]. \end{aligned} \quad (26)$$

From the above equations, we can notice that the extrinsic LLR expressions are the same for all three equalizers. In other words, for all iterations, the means (and the variances) are the same for all three equalizers. Hence, in equalizers I and II, the extrinsic LLR calculation is able to compensate for the bias introduced by the equalizer. However, since the symbol decision is taken at the equalizer output (i.e., before the LLR updating), a residual bias will be present at the final symbol estimates of equalizers I and II. Anyway, for equalizer II, the residual bias only contains a positive scaling factor that does not affect the QPSK BER, which therefore is the same as the BER of the unbiased equalizer III. On the contrary, for equalizer I, the residual bias also contains an additive term that produces a BER performance loss with respect to equalizers II and III.

The equivalence between the extrinsic LLRs for the biased equalizer II and the unbiased equalizer III is a nice result, because it establishes a clear link with noniterative equalizers, for which it is well known that biased and unbiased equalizers are equivalent, for constant-modulus constellations. This also justifies the use of the biased MMSE equalizer, instead of the unbiased one, in other turbo scenarios, e.g., those in [19], [20], and [22]. We remark that, in general, the equivalence between biased and unbiased equalizers does not hold for nonconstant-modulus constellations, e.g., 16-QAM. An example of this behavior has already been shown in [21], where an unbiased minimum variance (i.e., unbiased MMSE) equalizer outperforms the biased MMSE equalizer. It is worth noting that the unbiased MMSE equalizer of [21] has been derived using interference cancellation, i.e., in a different way with respect to our equalizer. When also channel coding is incorporated into the turbo loop, our unbiased equalizer III can be interpreted as the corresponding version of [21] for OFDM communications over time-varying channels.

Note that the proposed iterative BLE's also have their serial counterparts, as for instance discussed in [10]. In the serial case, the equalizer is updated from subcarrier to subcarrier and a different matrix inverse has to be computed for each subcarrier, which actually could be carried out in a recursive fashion as explained in [20]. The advantage of this subcarrier by subcarrier processing is that one can choose between updating the priors from one subcarrier to the next (sequential iterative estimation (SIE) in [10]) or from one OFDM symbol to the next (block iterative estimation (BIE) in [10]). On the contrary, the proposed iterative BLE's remain fixed for the entire OFDM symbol, since the matrix inverse contained in $\mathbf{G}$ is the same for all the subcarriers. Therefore, we can only update our priors from one OFDM-symbol iteration to the next.

V. Low-Complexity Algorithms

In this section, we investigate the computational complexity of the proposed equalizers. Our aim is to show some useful expedients that render this complexity linear in the number of active subcarriers N_A.

In order to calculate $\hat{s}_i$ in (6), (17), and (23), and t_i in (10), a matrix inverse $\mathbf{A^{-1}}$ is required. The standard computation of a matrix inverse requires a complexity of $O\left(N_A^3\right)$, which is too much for an OFDM system, even with a moderate number of active subcarriers. However, [9], [11] show how to exploit the banded structure of the approximated frequency-domain channel matrix $\mathbf{B}$ to reduce complexity. Specifically, instead of computing the matrix inverse, the equalization is performed by applying a band LDL^H factorization [28] to the matrix to be inverted, as expressed by

$$\mathbf{A} = \mathbf{BVB}^H + \mathbf{R_n} = \mathbf{LDL}^H \tag{27}$$

where $\mathbf{L}$ is a unit lower triangular matrix and $\mathbf{D}$ is diagonal, followed by a linear system solver that exploits this matrix decomposition to solve (6), (17), and (23) in one step for all i's. Instead of inverting the matrix $\mathbf{A}$ in (27), we solve the linear system $\mathbf{Ac} = \mathbf{b}$, which can be written as $\mathbf{LDL}^H\mathbf{c} = \mathbf{b}$ by (27). As explained in [9], this can be solved in three steps: first, $\mathbf{Lc}' = \mathbf{b}$ is solved for $\mathbf{c}'$, then $\mathbf{Dc}'' = \mathbf{c}'$ is solved for $\mathbf{c}''$, and eventually $\mathbf{L}^H\mathbf{c} = \mathbf{c}''$ is solved for $\mathbf{c}$. Overall, this leads to a complexity of $O(N_A)$. Note that this is valid only when the frequency-domain noise covariance matrix $\mathbf{R_n}$ is banded. In this paper, we adopt the minimum band-approximation-error sum-of-exponentials (MBAE-SOE) windows [11], which are able to fulfill the banded constraint of the frequency-domain noise covariance matrix.

Although solving a banded linear system requires a complexity that is only linear in N_A, this is not sufficient to guarantee that the full equalization procedure presented in the previous section has a linear complexity. Indeed, for all equalizers, we also need to calculate $t_i = \mathbf{b}_i^H\mathbf{A}^{-1}\mathbf{b}_i$ for each subcarrier i. Intuitively, a linear system solver for $\mathbf{Ac}_i = \mathbf{b}_i$ based on the band LDL^H factorization of $\mathbf{A}$, should be repeated for each subcarrier, leading to a complexity that is quadratic in N_A. Similarly, exploiting the banded structure of $\mathbf{A}$, an explicit calculation of the inverse $\mathbf{A}^{-1}$ would also require a quadratic complexity [29].

To reduce the complexity of the t_i calculations from quadratic to linear, we exploit the fact that the vector $\mathbf{b}_i$ is the ith column of the banded matrix $\mathbf{B}$, which is characterized by $2Q+1$ nonzero diagonals. This means that $\mathbf{b}_i$ has only $2Q+1$ nonzero elements, from $i-Q$ to $i+Q$. Since these nonzero elements are contiguous, we will refer to $\mathbf{b}_i$ as a *banded vector*. Hence, to calculate a specific $t_i = \mathbf{b}_i^H\mathbf{A}^{-1}\mathbf{b}_i$, we only need a square subblock of $\mathbf{A}^{-1}$ of dimension $2Q+1$. More specifically, by defining $\mathbf{P} = \mathbf{A}^{-1}$, only the $4Q+1$ diagonals in the main band of $\mathbf{P}$ are necessary in order to calculate the t_i values (see Fig. 3). Now, we split the complexity calculation in two parts: computing the main band of $\mathbf{P}$, and computing the t_i values from the knowledge of the main band of $\mathbf{P}$.

The calculation of the main band of $\mathbf{P}$ can be done from the band LDL^H factorization of $\mathbf{A}$, which is already available, with complexity $O(N_A)$ [29]. Let us define $p_{i,j}$ as the (i,j)th element of $\mathbf{P}$, $l_{i,j}$ as the $(i,\ j)$th element of $\mathbf{L}$, and $d_{i,i}$ as the $(i,\ i)$th element of $\mathbf{D}$. The algorithm starts from calculating p_{N_A,N_A}, which is at the bottom right corner of $\mathbf{P}$, and then calculates the elements from the bottom to the top. Within each row, each element is calculated from the right to the left. The algorithm is adapted from [29], and is summarized in Table II.

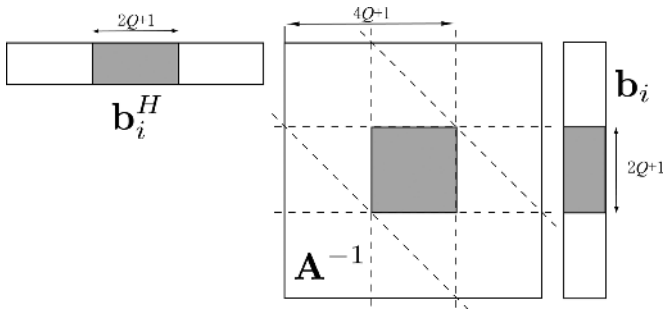

Fig. 3. Structure of t_i.

TABLE II
Calculation of the Main Band of $\mathbf{P}$

$p_{N_A,N_A} = 1/d_{N_A,N_A}$
for $i = (N_A-1):(-1):1$
  $M_i = \min(N_A, i+2Q)$
  for $j = M_i:(-1):(i+1)$
    $p_{i,j} = -\sum_{k=i+1}^{M_i} l_{k,i}^* p_{k,j}$
    $p_{j,i} = p_{i,j}^*$
  end
  $p_{i,i} = 1/d_{i,i} - \sum_{k=i+1}^{M_i} l_{k,i} p_{i,k}$
end

Let us now evaluate the complexity of the algorithm described above. Calculating the main band of $\mathbf{P}$ requires $(4Q^2+2Q)(N_A-1)$ complex multiplications (CM), $(4Q^2+2Q)(N_A-1)$ complex additions (CA) and N_A complex divisions (CD). The computation of each t_i requires $(2Q+1)(2Q+2)$ CM and $2Q(2Q+2)$ CA. Hence, in total, approximately $(8Q^2+8Q+2)N_A$ CM, $(8Q^2+6Q)N_A$ CA and N_A CD are needed to calculate all the t_i's.

For the complexity of the block turbo equalizer I, we use the results of [11], and we observe that computing (6) requires $(4Q^2+16Q+6)N_A$ CM, $(4Q^2+12Q+3)N_A$ CA and $(2Q+1)N_A$ CD. Calculating the extrinsic information in (11) requires $6N_A$ CM, $2N_A$ CA and $2N_A$ CD. Updating the soft information in (12) requires N_A CM, $3N_A$ CA, N_A CD, and $2N_A$ hyperbolic tangent calculations. The hyperbolic tangent function can be evaluated by using a lookup table or a low-complexity numerical algorithm. The complexity analysis of the other block turbo equalizers is similar to that of equalizer I. Table III gives a comprehensive overview of the complexity of a generic iteration for the three block turbo equalizers. Please observe that the complexity of the first iteration is even smaller, because the prior means m_i and variances v_i are 0 and 1, respectively, and hence some additions and multiplications can be omitted. Summarizing, the proposed block turbo MMSE equalizers are characterized by a low complexity, which is linear in the number of active subcarriers N_A. A complexity analysis of the SIE/BIE has

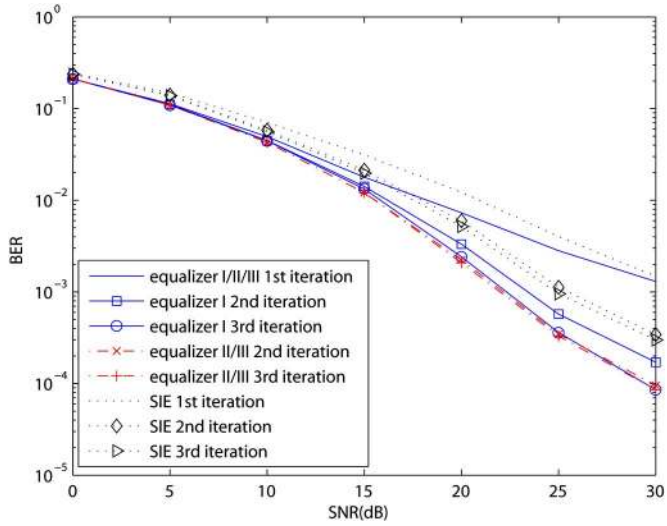

Fig. 4. BER comparison of equalizer I/II/III and SIE, uniform power delay profile.

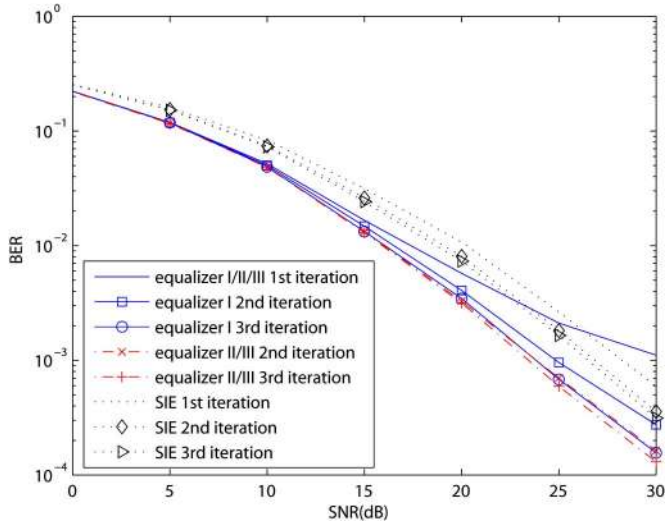

Fig. 5. BER comparison of equalizer I/II/III and SIE, exponential power delay profile.

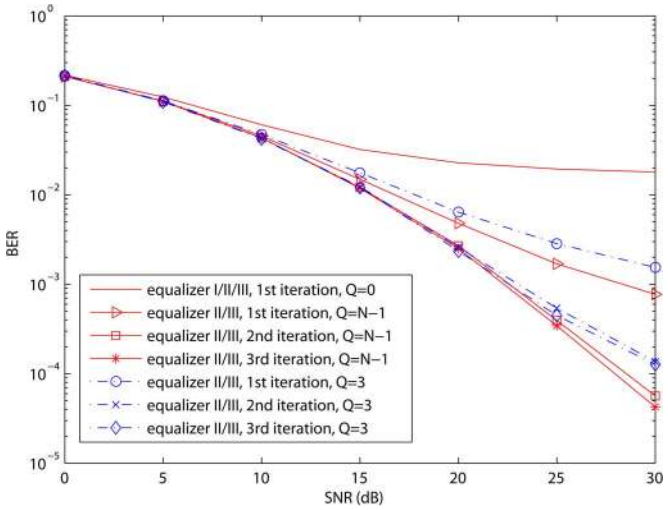

Fig. 6. BER reference for equalizer II/III, uniform power delay profile.

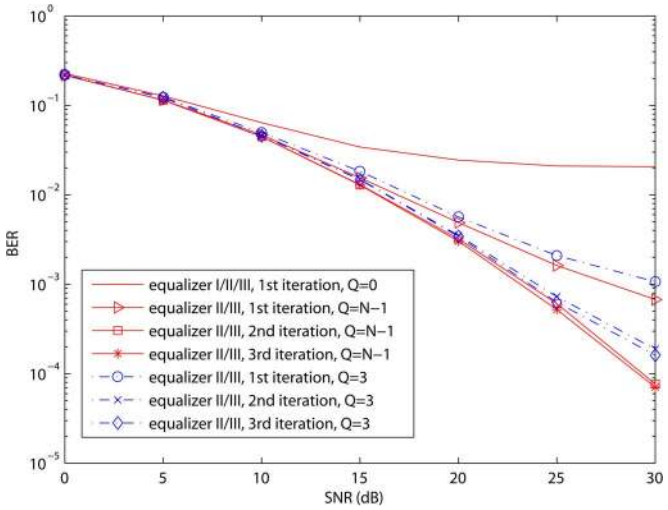

Fig. 7. BER reference for equalizer II/III, exponential power delay profile.

been derived in [9], which showed similar $O\left(Q^2 N_A\right)$ computational complexity. However, in the next section we demonstrate that the proposed block turbo MMSE equalizers have a performance advantage over the SIE/BIE.

VI. Simulation Results

In this section, the proposed algorithms are examined and compared by simulations. We consider an OFDM system with $N = 128$ subcarriers, $N_A = 96$ of which are active. The maximum channel delay spread and the CP length are the same and equal to $L = 32$. We denote with $h_{n,l}$ the lth channel tap at the nth time instant. The channel is assumed to be Rayleigh distributed with uniform $E\left\{|h_{n,l}|^2\right\} = 1/L$ or exponential $E\left\{|h_{n,l}|^2\right\} = e^{-0.6l}/\sum_{l'=1}^{L} e^{-0.6l'}$ power delay profile, and a U-shaped Doppler spectrum. As indicated before, the unbiased equalizer III has the same BER performance as the biased equalizer II for constant-modulus constellations such as the QPSK used in our simulation.

We consider a high-mobility case where the normalized Doppler frequency is $f_d/\Delta f = 0.15$ with f_d the Doppler frequency and Δf the subcarrier spacing. As indicated in [2], the subcarrier spacing is approximately 4464/2232/1116 Hz for the 2K/4K/8K mode operation in DVB-H. The Doppler frequency f_d can be as high as 120 Hz corresponding to a speed of 160km/h @ 800 MHz (upper part of Band V) to 650km/h @ 200 MHz (lower part of band III). Such a speed range could cover most of the vehicle and high-speed train velocities.

Figs. 4 and 5 compare the BER performances of equalizers I, II and III with the SIE of [10], in channels with uniform and exponential power-delay profile, respectively. We do not compare with the BIE of [10], since it has a worse performance than the SIE. The time-domain receiver window is designed for a bandwidth parameter $Q = 3$. As a reference, the BER performances of the traditional receiver $(Q = 0)$ and the nonbanded MMSE receiver $(Q = N-1)$ are also shown in Figs. 6 and 7, for a uniform and exponential power delay profile, respectively. It can be seen that with $Q = 3$, the banded equalizers are very close to the nonbanded MMSE equalizer $(Q = N-1)$.

The simulation results in Figs. 4–7 show that the block turbo equalizer outperforms the serial turbo equalizer. This result, which corroborates our initial expectation, is mainly due to the

TABLE III
COMPLEXITY ANALYSIS

	CA	CM	CD	tanh
equalizer I	$(12Q^2+18Q+8)N_A$	$(12Q^2+24Q+15)N_A$	$(2Q+5)N_A$	$2N_A$
equalizers II and III	$(12Q^2+18Q+10)N_A$	$(12Q^2+24Q+17)N_A$	$(2Q+7)N_A$	$2N_A$

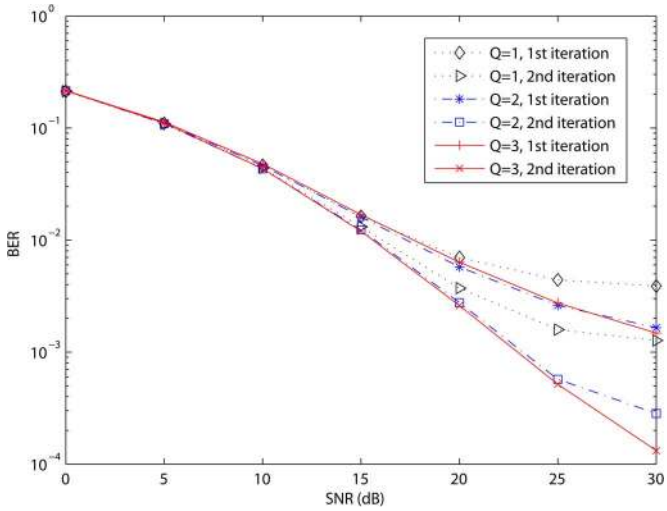

Fig. 8. BER performance of equalizer II/III for different Q's.

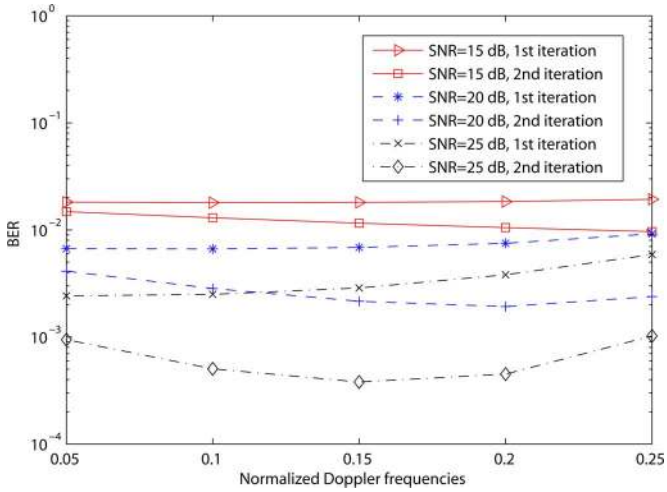

Fig. 9. BER performance of equalizer II/III for different normalized Doppler frequencies.

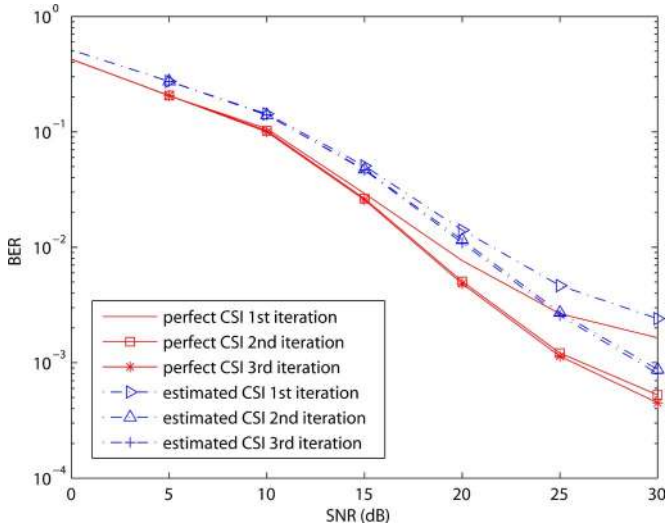

Fig. 10. BER performance of equalizer II/III under channel estimation uncertainties.

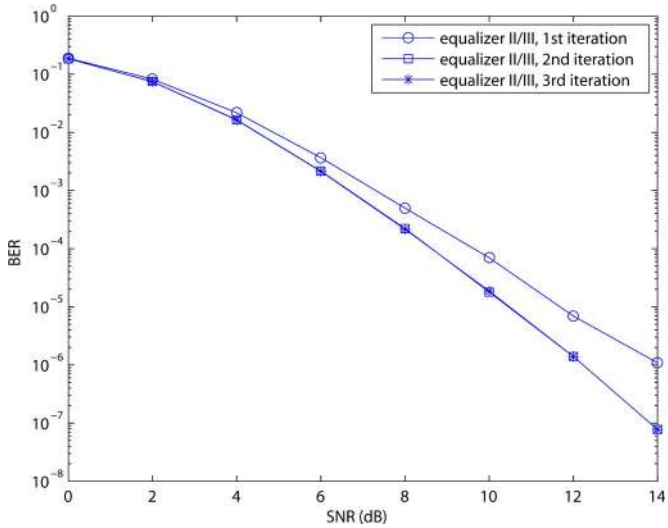

Fig. 11. BER performance of equalizer II/III with error correction coding.

window design, which is done over the entire OFDM block. Further, we observe that both methods converge slowly after two iterations. In the first iteration, when no *a priori* information is available, equalizers I, II, and III have the same performance since they are simply the standard MMSE BLE of [11]. Because of the additive term into its residual bias, equalizer I produces worse BER performance than equalizers II and III. All the banded equalizers have an error floor due to the band approximation error of the channel. The error floor can be decreased by increasing the bandwidth parameter Q, as shown in Fig. 8 for the uniform power delay profile.

We have also tested our equalizers for various normalized Doppler frequencies ranging from $f_d/\Delta f = 0.05$ to $f_d/\Delta f = 0.25$. We assume a uniform power delay profile and $L = 32$ with bandwidth parameter $Q = 3$. The BER performance curves are rather flat as a function of $f_d/\Delta f$, as shown in Fig. 9 for some specific SNRs. These results testify that our algorithms are robust to different Doppler spreads.

Fig. 10 shows the BER performance of equalizer II/III when CSI is not available at the receiver. The pilot-assisted time-varying MMSE channel estimator [23] is employed, using the

discrete Karhunen–Loève basis expansion model [31]. We assume a uniform power delay profile and $L = 6$, with normalized Doppler frequency $f_d/\Delta f = 0.15$ and $Q = 3$. We only take $L = 6$ since for a system with large L, channel estimation over multiple OFDM blocks is required [30] in order to have a high spectral efficiency. Among the $N = 128$ subcarriers, 98 subcarriers are used for data, whereas the remaining 30 are reserved for pilots, which are grouped into six equidistant clusters, each having five pilot tones. The average power of the pilot subcarriers is the same as the power of the data subcarriers. Simulation results show the validity of the equalization algorithm under channel estimation.

Finally, we show that the BER performance can be further improved by incorporating error correction coding as present in all communication standards. We use similar parameters as in [19]. A rate 1/2 convolutional code with generator matrix $[101; 111]$ and a block length of 2^{15} is used. The uniform power delay profile is used, with $f_d/\Delta f = 0.15$, $L = 32$ and $Q = 3$. We employ random interleaving. The decoder employs a linear approximation to the log-MAP decoding algorithm. The receiver is assumed to have perfect CSI. Fig. 11 shows that at high SNR, nearly 2-dB gain can be achieved through turbo equalization.

VII. Conclusion

We have proposed low-complexity MMSE block turbo equalizers for OFDM systems in time-varying channels. By exploiting the banded structure of the frequency-domain channel matrix, as well as receiver windowing to enforce this band assumption, the complexity of the equalizers is linear in the number of subcarriers. We have derived turbo equalizers operating on the entire OFDM symbol, showing better performance than the serial turbo equalizer. Three turbo equalizers have been proposed. The first and second are both based on a biased MMSE criterion. The difference between these two equalizers is that the first does not achieve independence between the extrinsic and *a priori* information, whereas the second does.

$$
\begin{aligned}
L_e(s_{i,1}) &= \ln \frac{p(\hat{s}_i|s_i=\alpha_1)P(0)+p(\hat{s}_i|s_i=\alpha_3)P(1)}{p(\hat{s}_i|s_i=\alpha_2)P(0)+p(\hat{s}_i|s_i=\alpha_4)P(1)} \\
&= \ln \frac{\exp\left(-\frac{|\hat{s}_i-\mu_{i,1}|^2}{\sigma_{i,1}^2}\right)P(0)+\exp\left(-\frac{|\hat{s}_i-\mu_{i,3}|^2}{\sigma_{i,3}^2}\right)P(1)}{\exp\left(-\frac{|\hat{s}_i-\mu_{i,2}|^2}{\sigma_{i,2}^2}\right)P(0)+\exp\left(-\frac{|\hat{s}_i-\mu_{i,4}|^2}{\sigma_{i,4}^2}\right)P(1)} \\
&= \ln \frac{\exp\left(-\frac{|[\hat{s}_i-m_i(1-v_it_i)]-v_it_i\alpha_1|^2}{\sigma_{i,1}^2}\right)P(0)+\exp\left(-\frac{|[\hat{s}_i-m_i(1-v_it_i)]-v_it_i\alpha_3|^2}{\sigma_{i,3}^2}\right)P(1)}{\exp\left(-\frac{|[\hat{s}_i-m_i(1-v_it_i)]-v_it_i\alpha_2|^2}{\sigma_{i,2}^2}\right)P(0)+\exp\left(-\frac{|[\hat{s}_i-m_i(1-v_it_i)]-v_it_i\alpha_4|^2}{\sigma_{i,4}^2}\right)P(1)} \\
&= \ln \frac{\exp\left(\frac{2\mathrm{Re}\{[\hat{s}_i-m_i(1-v_it_i)]^*\cdot v_it_i\alpha_1\}}{\sigma_{i,1}^2}\right)P(0)+\exp\left(\frac{2\mathrm{Re}\{[\hat{s}_i-m_i(1-v_it_i)]^*\cdot v_it_i\alpha_3\}}{\sigma_{i,3}^2}\right)P(1)}{\exp\left(\frac{2\mathrm{Re}\{[\hat{s}_i-m_i(1-v_it_i)]^*\cdot v_it_i\alpha_2\}}{\sigma_{i,2}^2}\right)P(0)+\exp\left(\frac{2\mathrm{Re}\{[\hat{s}_i-m_i(1-v_it_i)]^*\cdot v_it_i\alpha_4\}}{\sigma_{i,4}^2}\right)P(1)}.
\end{aligned} \tag{28}
$$

$$
\begin{aligned}
L_e(s_{i,1}) &= \ln \frac{\exp\left(\frac{2\mathrm{Re}\{c\alpha_1\}}{\sigma_{i,1}^2}\right)P(0)+\exp\left(\frac{2\mathrm{Re}\{c\alpha_3\}}{\sigma_{i,3}^2}\right)P(1)}{\exp\left(\frac{2\mathrm{Re}\{c\alpha_2\}}{\sigma_{i,2}^2}\right)P(0)+\exp\left(\frac{2\mathrm{Re}\{c\alpha_4\}}{\sigma_{i,4}^2}\right)P(1)} \\
&= \ln \frac{\exp\left(\frac{\sqrt{2}}{\sigma_{i,1}^2}\mathrm{Re}\{c(1+j)\}\right)P(0)+\exp\left(\frac{\sqrt{2}}{\sigma_{i,3}^2}\mathrm{Re}\{c(1-j)\}\right)P(1)}{\exp\left(\frac{\sqrt{2}}{\sigma_{i,2}^2}\mathrm{Re}\{c(-1+j)\}\right)P(0)+\exp\left(\frac{\sqrt{2}}{\sigma_{i,4}^2}\mathrm{Re}\{c(-1-j)\}\right)P(1)} \\
&= \ln \frac{\exp\left(\frac{\sqrt{2}}{\sigma_{i,1}^2}[\mathrm{Re}\{c\}-\mathrm{Im}\{c\}]\right)P(0)+\exp\left(\frac{\sqrt{2}}{\sigma_{i,3}^2}[\mathrm{Re}\{c\}+\mathrm{Im}\{c\}]\right)P(1)}{\exp\left(\frac{\sqrt{2}}{\sigma_{i,2}^2}[-\mathrm{Re}\{c\}-\mathrm{Im}\{c\}]\right)P(0)+\exp\left(\frac{\sqrt{2}}{\sigma_{i,4}^2}[-\mathrm{Re}\{c\}+\mathrm{Im}\{c\}]\right)P(1)} \\
&= \ln\left[\exp\left(\frac{2\sqrt{2}}{\sigma_{i,1}^2}\mathrm{Re}\{c\}\right)\right] \\
&= \frac{2\sqrt{2}}{\sigma_{i,1}^2}\mathrm{Re}\{[\hat{s}_i-m_i(1-v_it_i)]^*v_it_i\} \\
&= \frac{\sqrt{8}\mathrm{Re}(\hat{s}_i-m_i(1-v_it_i))}{v_i(1-v_it_i)},
\end{aligned} \tag{29}
$$

Simulation results show that introducing this independence reduces the error floor. The third equalizer, on the other hand, is based on the unbiased MMSE criterion and is equivalent to the second equalizer for constant-modulus constellations. Error correction codes have also been included to further improve the performance. As an example, we have shown some simulation results in the presence of channel estimation errors. Future research could aim at improving the performance of channel estimation. This could be done by exchanging the soft information between the channel estimator and the equalizer to improve the system performance, e.g., under the framework proposed by [24] for single-carrier communications.

APPENDIX
DERIVATION OF EXTRINSIC INFORMATION

For simplicity, we only derive the expression of $L_e(s_{I,i,1})$ in (11). The derivation of $L_e(s_{I,i,2})$ is similar. We define $P(0) = P(s_{I,i,2} = 0)$ and $P(1) = P(s_{I,i,2} = 1)$, and omit the subscript I. From (5), we can derive $L_e(s_{i,1})$ as in (28) shown at the bottom of the previous page. Defining $c = [\hat{s}_i - m_i(1 - v_i t_i)]^* v_i t_i$, we can further simplify (28), as illustrated in (29) shown at the bottom of the previous page, where we have used the fact that all the $\sigma^2_{i,k}$, $k = 1, \ldots, 4$ have the same value.

REFERENCES

[1] R. van Nee and R. Prasad, *OFDM For Wireless Multimedia Communications*. Norwood, MA: Artech House, Jan. 2000.

[2] G. Faria, J. A. Henriksson, E. Stare, and P. Talmola, "DVB-H: Digital broadcasting sevices to handheld devices," *Proc. IEEE*, vol. 94, pp. 194–209, Jan. 2006.

[3] Z. Wang and G. B. Giannakis, "Wireless multicarrier communications: Where fourier meets shannon," *IEEE Signal. Process. Mag.*, vol. 17, no. 3, pp. 29–48, May 2000.

[4] T. Wang, J. Proakis, E. Masry, and J. Zeidler, "Performance degradation of OFDM system due to Doppler spreading," *IEEE Trans. Wireless Commun.*, vol. 5, no. 6, pp. 1422–1432, Jun. 2006.

[5] I. Barhumi, G. Leus, and M. Moonen, "Equalization for OFDM over doubly-selective channels," *IEEE Trans. Signal Process.*, vol. 54, no. 4, pp. 1445–1458, Apr. 2006.

[6] A. Stamoulis, S. N. Diggavi, and N. Al-Dhahir, "Intercarrier interference in MIMO OFDM," *IEEE Trans. Signal Process.*, vol. 50, no. 10, pp. 2451–2464, Oct. 2002.

[7] X. Huang and H.-C. Wu, "Robust and efficient intercarrier interference mitigation for OFDM systems in time-varying fading channels," *IEEE Trans. Veh. Technol.*, vol. 56, no. 5, pp. 2517–2528, Sep. 2007.

[8] W. G. Jeon, K. H. Chang, and Y. S. Cho, "An equalization technique for orthogonal frequency-division multiplexing systems in time-variant multipath channels," *IEEE Trans. Commun.*, vol. 47, no. 1, pp. 27–32, Jan. 1999.

[9] L. Rugini, P. Banelli, and G. Leus, "Simple equalization of time-varying channels for OFDM," *IEEE Commun. Lett.*, vol. 9, no. 7, pp. 619–621, Jul. 2005.

[10] P. Schniter, "Low-complexity equalization of OFDM in doubly-selective channels," *IEEE Trans. Signal Process.*, vol. 52, no. 4, pp. 1002–1011, Apr. 2004.

[11] L. Rugini, P. Banelli, and G. Leus, "Low-complexity banded equalizers for OFDM systems in Doppler spread channels," *EURASIP J. Appl. Signal Process.*, vol. 2006, pp. 1–13, 2006, Article ID 67404.

[12] A. Gorokhov and J. P. Linnartz, "Robust OFDM receivers for dispersive time-varying channels: Equalization and channel acquisition," *IEEE Trans. Commun.*, vol. 52, no. 4, pp. 572–583, Apr. 2004.

[13] Y.-S. Choi, P. J. Voltz, and F. A. Cassara, "On channel estimation and detection for multicarrier signals in fast and selective rayleigh fading channels," *IEEE Trans. Commun.*, vol. 49, no. 8, pp. 1375–1387, Aug. 2001.

[14] X. Cai and G. B. Giannakis, "Bounding performance and suppressing intercarrier interference in wireless mobile OFDM," *IEEE Trans. Commun.*, vol. 51, no. 12, pp. 2047–2056, Dec. 2003.

[15] S. Tomasin, A. Gorokhov, H. Yang, and J.-P. Linnartz, "Iterative interference cancellation and channel estimation for mobile OFDM," *IEEE Trans. Wireless Commun.*, vol. 4, no. 1, pp. 238–245, Jan. 2005.

[16] Y. Zhao and S.-G. Haggman, "Intercarrier interference self-cancellation scheme for OFDM mobile communication systems," *IEEE Trans. Commun.*, vol. 49, no. 7, pp. 1185–1191, Jul. 2001.

[17] S.-J. Hwang and P. Schniter, "Efficient sequence detection of multicarrier transmissions over doubly dispersive channels," *EURASIP J. Appl. Signal Process.*, vol. 2006, pp. 1–17, 2006, Article ID 93638.

[18] S. Ohno, "Maximum likelihood inter-carrier interference suppression for wireless OFDM with null subcarriers," in *Proc. Int. Conf. Acoust., Speech, Signal Process. (ICASSP)*, Mar. 2005, vol. 3, pp. 849–852.

[19] M. Tüchler, R. Koetter, and A. C. Singer, "Turbo equalization: Principles and new results," *IEEE Trans. Commun.*, vol. 50, no. 5, pp. 754–767, May 2002.

[20] M. Tüchler, A. C. Singer, and R. Koetter, "Minimum mean squared error equalization using *a priori* information," *IEEE Trans. Signal Process.*, vol. 50, no. 3, pp. 673–683, Mar. 2002.

[21] M. A. Dangl, C. Sgraja, and J. Lindner, "An improved block equalization scheme for uncertain channel estimation," *IEEE Trans. Wireless Commun.*, vol. 6, no. 1, pp. 146–156, Jan. 2007.

[22] X. Wang and H. Poor, "Iterative (turbo) soft interference cancellation and decoding for coded CDMA," *IEEE Trans. Commun.*, vol. 47, no. 7, pp. 1046–1061, Jul. 1999.

[23] Z. Tang, R. C. Cannizzaro, G. Leus, and P. Banelli, "Pilot-assisted time-varying channel estimation for OFDM systems," *IEEE Trans. Signal Process.*, vol. 55, no. 5, pp. 2226–2238, May 2007.

[24] R. Otnes and M. Tüchler, "Iterative channel estimation for turbo equalization of time-varying frequency-selective channels," *IEEE Trans. Wireless Commun.*, vol. 3, pp. 146–156, Nov. 2004.

[25] H. V. Poor, *An Introduction to Signal Detection and Estimation*, 2nd ed. New York: Springer-Verlag, 1994, pp. 221–229.

[26] H. V. Poor and S. Verdu, "Probability of error in MMSE multiuser detection," *IEEE Trans. Inf. Theory*, vol. 43, no. 3, pp. 858–871, May 1997.

[27] J. M. Cioffi, G. P. Dudevoir, M. V. Eyuboglu, and G. D. Forney, "MMSE decision-feedback equalizers and coding—Part I: Equalization results," *IEEE Trans. Commun.*, vol. 43, no. 10, pp. 2582–2594, Oct. 1995.

[28] T. K. Moon and W. C. Stirling, *Mathematical Methods and Algorithms For Signal Processing*. Englewood Cliffs, NJ: Prentice-Hall, 2000.

[29] A. Asif and J. M. F. Moura, "Block matrices with l -block-banded inverse: Inversion algorithms," *IEEE Trans. Signal Process.*, vol. 53, no. 2, pp. 630–642, Feb. 2005.

[30] Z. Tang, G. Leus, and P. Banelli, "Pilot-assisted time-varying OFDM channel estimation based on multiple OFDM symbols," in *Proc. Workshop on Signal Processing Advances in Wireless Communications (SPAWC)*, Cannes, France, Jul. 2006.

[31] M. Visintin, "Karhunen-Loeve expansion of a fast Rayleigh fading process," *IEEE Electron. Lett.*, vol. 32, pp. 1712–1713, Aug. 1996.

Kun Fang (S'06) was born in Tianjin, China, on January 5, 1981. He received the B.E. degree in electrical engineering from the University of Science and Technology of China in 2003, and the M.S. degree in electrical engineering from the Swiss Federal Institute of Technology (ETH), Zurich, Switzerland, in 2005. Since then, he has been working towards the Ph.D. degree at the Circuit and Systems group, Delft University of Technology, Delft, The Netherlands.

His research interests are in the area of signal processing for communications.

Luca Rugini (M'05) was born in Perugia, Italy, in 1975. He received the Laurea degree in electronic engineering and the Ph.D. degree in telecommunications from the University of Perugia, in 2000 and 2003, respectively.

From February to July 2007, he visited Delft University of Technology, The Netherlands. He is currently a Postdoctoral Researcher with the Department of Electronic and Information Engineering at the University of Perugia. His research interests lie in the area of signal processing for multicarrier and spread-spectrum communications.

Geert Leus (SM'05) was born in Leuven, Belgium, in 1973. He received the Electrical Engineering degree and the Ph.D. degree in applied sciences from the Katholieke Universiteit Leuven, Leuven, Belgium, in 1996 and 2000, respectively.

He has been a Research Assistant and a Postdoctoral Fellow of the Fund for Scientific Research-Flanders, Belgium, from October 1996 until September 2003. During that period, he was with the Electrical Engineering Department, the Katholieke Universiteit Leuven. Currently, he is an Associate Professor at the Faculty of Electrical Engineering, Mathematics and Computer Science, Delft University of Technology, Delft, The Netherlands. During summer 1998, he visited Stanford University, Stanford, CA, and from March 2001 until May 2002 he was a Visiting Researcher and Lecturer at the University of Minnesota. His research interests are in the area of signal processing for communications.

Dr. Leus received a 2002 IEEE Signal Processing Society Young Author Best Paper Award and a 2005 IEEE Signal Processing Society Best Paper Award. He is a member of the IEEE Signal Processing for Communications Technical Committee and an Associate Editor for the IEEE TRANSACTIONS ON SIGNAL PROCESSING and the *EURASIP Journal on Applied Signal Processing*. In the past, he has served on the Editorial Board of the IEEE SIGNAL PROCESSING LETTERS and the IEEE TRANSACTIONS ON WIRELESS COMMUNICATIONS.